Author's Response

Part-I: A point-by-point response

These responses were to integrate comments from the public referees and further explanations from authors.

1. Title: "...GHG concentrations from agricultural soils" - you measure GHG concentrations in ambient air above ground surface - these concentrations can stem from emissions from the soil (including roots and microorganisms) or from the above ground vegetation. You do not measure fluxes - so be careful within your introduction - to estimate fluxes the concentration is only one of the variables needed!!!

   Response: I would modify this title to 'Application of Open Path Fourier Transform Infrared Spectroscopy (OP-FTIR) to Measure Greenhouse Gas Concentrations from Agricultural Fields'

2. Page 2, line 10 ff: The authors mention chamber measurements as the most common way to investigate emissions from soils. In the same time they point out the relatively small footprint as the main limit of this method. However, I would like to introduce in this context the opportunity to measure GHG fluxes on larger scale using the Eddy Covariance flux measurements. This method is also an established method nowadays and a common micro-meteorological technique with an increased footprint to determine emissions for instance of CO_2, CH_4 and water from soils and vegetation. (e.g., Baldocchi, D. (2003): Assessing the eddy covariance technique for evaluating carbon dioxide exchange rates of ecosystems: past, present and future. https://doi.org/10.1046/j.1365-2486.2003.00629.x). Concerning to comment No. 1 - all methods are based on the measurement of the concentrations of GHGs and have their own processes to obtain emission rates.

   Response: It is a good idea to point out the eddy covariance and its advantage (e.g., larger footprint) for gas flux measurements. I would briefly introduce this method into the context. Chamber measurements are the most common method for soil gas emission measurements because this method also provides numbers of strengths. One of the advantages is that chambers are sensitive enough to make comparisons of gas emissions in different treatments (e.g., field and N management practices in small plots (< 3 ha)), which is challenging to the eddy covariance. The OP-FTIR combined with inversion dispersion techniques (e.g., backward Lagrangian stochastic dispersion model) is capable of measuring gas emissions frequently and with a field-scale footprint (1-3 ha), that can both compensate the limitations of chamber measurements and measure gas emissions from different treatment plots. That is the reason why eddy covariance was not introduced in the context in the first place.

3. In section 2.3 (Page 5, line 17), two anonymous referees suggested further explaining the rationality of "Ninety spectra containing 338±0.3 ppbv N_2O and ninety-three spectra containing 400±3.0 ppmv CO_2 were selected from these valid spectra to calculate concentrations of N_2O and CO_2, respectively, using different quantitative methods."

Response: The S-OPS and OP-FTIR were deployed at the same path to measure the path-averaged N_2O/CO_2 concentrations and collect OP-FTIR spectra simultaneously. Ninety FTIR spectra containing N_2O concentrations from 337.4 – 338.5 ppbv (measured by the S-OPS), and ninety-three spectra containing CO_2 concentrations from 405.4 – 394.9 ppmv (also measured by the S-OPS) were collected (see the following table) and quantified for N_2O/CO_2 concentrations using different quantification methods (including least square models, single beam (SB) backgrounds, and spectral windows). These spectra, containing consistent N_2O/CO_2 concentrations but different water vapour content and temperature, can be used to examine the sensitivity of quantification methods to water vapour and temperature. For instance, the variations in the FTIR-calculated concentrations (figure--5 and -6 shown in the manuscript) resulted from the confounding effects of ambient water vapor interferences and temperature.

Table - The S-OPS measured concentrations of N_2O/CO_2 used for OP-FTIR quantitative method evaluations.

Gases	Statistics of the S-OPS measured concentrations					
	Mean	SD	Max	Median	Min	n
N_2O (ppbv)	337.9	0.3	338.5	337.9	337.4	90
CO_2 (ppmv)	399.8	3.0	405.4	398.9	394.9	93

4. In section 2.3: How often did you acquire a single beam spectrum? (how many spectra did you measure during the operational period - also to make the number of 877 valid OP-FTIR spectra more valuable)?

Response: Gas samples were continuously collected from the S-OPS and measured for N_2O concentrations every 10 s using the difference frequency generation (DFG) mid-IR laser-based N_2O/H_2O analyzer (IRIS 4600). The measured N_2O concentrations were averaged every 30 min to represent the 'actual' ambient N_2O concentrations at the 30-min interval. Within the 30-min interval, the environment (e.g., gas concentrations, water vapour content, and temperature) was assumed stationary, meaning that the averaged quantities of variables were invariant. The 30-min averaged N_2O was used to benchmark the concentrations derived from the OP-FTIR spectra. A SB spectrum was collected every minute based on 64 sample scans. Within a 30-min interval, two to three SB spectra were collected and measured N_2O concentrations. The sampling time was shown in the following table. These two-three 'one-minute' N_2O concentrations were also averaged to calculate 30-min averaged N_2O to compare with the SOPS-measured concentrations. The whole OP-FTIR spectra used in this study should be 793 spectra rather than 877.

Table – An example of the timing for measuring N_2O concentrations using the S-OPS (SOPS-N2O) and for acquiring the OP-FTIR single beam (SB) spectra (FTIR-N_2O) on 9 Jun. 2014

Time of SOPS-N_2O (UTC)	Time of FTIR-N_2O (UTC)	Time of SOPS-N_2O (UTC)	Time of FTIR-N_2O (UTC)
06/09/2014 16:00	06/09/2014 15:37	06/09/2014 22:00	06/09/2014 21:33
	06/09/2014 15:39		06/09/2014 21:58
06/09/2014 16:30	06/09/2014 16:02		06/09/2014 21:59
	06/09/2014 16:03	06/09/2014 22:30	06/09/2014 22:22
	06/09/2014 16:28		06/09/2014 22:24
06/09/2014 17:00	06/09/2014 16:53	06/09/2014 23:00	06/09/2014 22:49
	06/09/2014 16:55	06/09/2014 23:30	06/09/2014 23:13
06/09/2014 17:30	06/09/2014 17:18		06/09/2014 23:15
	06/09/2014 17:19	06/10/2014 00:00	06/09/2014 23:40
06/09/2014 18:00	06/09/2014 17:44	06/10/2014 00:30	06/10/2014 00:05
06/09/2014 18:30	06/09/2014 18:09		06/10/2014 00:29
	06/09/2014 18:10	06/10/2014 01:00	06/10/2014 00:31
06/09/2014 19:00	06/09/2014 18:35		06/10/2014 00:56
06/09/2014 19:30	06/09/2014 19:00	06/10/2014 01:30	06/10/2014 01:20
	06/09/2014 19:01	06/10/2014 02:00	06/10/2014 01:45
	06/09/2014 19:25		06/10/2014 01:47
	06/09/2014 19:26	06/10/2014 02:30	06/10/2014 02:12
06/09/2014 20:00	06/09/2014 19:51	06/10/2014 03:00	06/10/2014 02:36
06/09/2014 20:30	06/09/2014 20:16		06/10/2014 02:38
	06/09/2014 20:17	06/10/2014 03:30	06/10/2014 03:01
06/09/2014 21:00	06/09/2014 20:42		06/10/2014 03:03
06/09/2014 21:30	06/09/2014 21:07		06/10/2014 03:28
	06/09/2014 21:08	06/10/2014 04:00	06/10/2014 03:53

5. In section 2.4, the authors stated that "each sampled spectrum was acquired by co-adding 64 single-sided interferograms (IFGs) at the nominal resolution of 0.5 cm^{-1}, which accounted for 32,000 data points were collected with an interval of 0.241 wavenumbers between data points, …" For interferograms, the unit of the interval of data points is cm, not wavenumber.

Response: This sentence might be confused. It means that a resolution of 0.5 cm^{-1} accounting for a data point every 0.241 wavenumbers was used for acquiring SB spectra (400 – 4000 cm^{-1}), and approximate 32,000 data points were in the interferogram.

6. In section 2.4, the authors employed some criteria to remove low-quality IFGs, which includes those of very intense centerburst. It is true that intense-centerburst IFGs result in severe non-linear response of MCT detectors. However, such IFGs have high signal-to-noise ratio, and would be valid once the non-linear detector response is corrected. The authors might be interested in correcting method (L. Shao, P.R. Griffiths, Anal. Chem., 2008, 80(13), 5219).

Response: The maximum A/DC capacity in this study was approximately 2.49 Volts. The optical path length of the OP-FTIR was 300 meters. The maximum or minimum value of the IFG centerburst in this study located between

0.61-1.14 volts, which prevented the MCT detector from saturation as well as avoided the non-linear response of the detector.

7. In section 2.5.1 (Page 6, line 23): I see the potential and limitation of the here discussed methods to obtain a target gas free background spectrum. In my opinion, using one background spectrum per day for the zap-bkg determination is to less due to the extensive impact of changing environmental conditions on the measured IR spectra (which is surely occurring during the day in ambient air conditions like air humidity, pressure variability, ...).

Response: Ideally, the zap-bkg spectrum needed to be created from each sample SB spectrum to obtain absorbance. In this study, however, we only created one zap-bkg spectrum for each day. This idea was inspired by the methodology of the zero-path SB spectrum used for absorbance spectra conversion. For continuous gas measurements, zero-path SB spectrum was usually acquired once per day and used to convert sample SB spectra to absorbance. Also, it is time-consuming to create the zap-bkg spectrum for each SB spectrum for continuous gas measurements. Yes, I would agree that this is the potential limitation of using the zap-bkg method and suggest that the future OP-FTIR users can test the effect of multiple zap-bkg on gas quantification before continuous gas measurements.

8. In section 2.5.1, the authors stated using "a high-order fitting function" as the synthetic background. It is better to be specific about the function, is it a quadratic, cubic polynomial, or something else?

Response: Numerous data points were selected from the field SB spectrum. A polynomial function was used to fit the field spectrum to synthesize the SB background without features of gas absorption.

9. In section 2.5.1 (Page 6, line 30): what is meant with: all data points are stored as one data file? You calculated from each SB spectra the synthetic background and store this in the same manner like the original data spectra and use these files for the calculation of abs-spectra? How many data points are used to determine the smooth background spectra function (which order of polynom).

Response: The idea of the synthetic SB background is to select multiple points from the sampled SB spectrum, and these selected points were used to fit the curvature of the SB spectrum using the polynomial function. The positions (or wavenumbers) of these selected points are important and need to be consistent for every sample SB spectrum. For instance, the positions must not be selected within the absorbance features. These data points were selected from a quality SB spectrum acquired from each day, and the wavenumbers of these selected data points were stored in one file (a data-point file is a feature provided by the IMACC software). A data-point file was applied in sample SB spectra to make sure the points applied in every sample SB spectrum have consistent positions. Six points

within 2050-2500 cm^{-1} were selected from the SB spectrum to smooth the SB background spectrum using polynomial function (six orders) (Figure 3b in the paper) for N_2O and CO_2 quantification.

10. In section 2.5.2, some useful information about PLS models is not provided, such as the number of calibration spectra (to build the model), the concentration range that the model covers, the number of factors for the model.

Response: Sixty mixed-gas (i.e., N_2O + water vapor) spectra were collected from the lab-based FTIR joined with the multi-pass gas cell (the optical path length of 33 meters). Concentrations of N_2O and water vapor ranged from 0.3 - 0.7 ppmv and 7000 – 30,000 ppmv, respectively. More details of the calibration spectra were shown in the supplementary table-2.

11. In section 2.6, it is better to be specific about the statistical tests, are they t-test or paired t-test?

Response: For N_2O analysis, twelve quantitative models used for N_2O concentration calculations from ninety OP-FTIR spectra were examined to optimize the combinations of SB backgrounds (i.e., zap- and syn-bkg), multivariate models (i.e., CLS and PLS), and analytical windows (i.e., W_N1-W_N4). In order to compare the means of the twelve populations, the Fisher's Least significant difference (LSD) was used for multiple comparisons ($\alpha = 0.05$). Likewise, the LSD was also used to compare six population means for the CO_2 analysis.

12. In section 3.2, the authors present the result of CLS (zap-bkg) and CLS (syn-bkg), and the result of PLS (syn-bkg). Why is the result of PLS (zap-bkg) absent? It seems that the authors did not apply PLS to estimate the concentrations of CO_2, as they did in case of N_2O. The reason should be explained.

Response: The syn-bkg is one of the recommended methods for converting the SB to absorbance spectra, but the zap-bkg was the newly proposed method. Thus, the syn-bkg was used to examine the feasibility and the performance of the zap-bkg. The identical field SB spectra, analytical windows, and CLS model were used to calculate gas concentrations from the absorbance spectra converted by zap- and syn-bkg. For both N_2O and CO_2 analyses, the zap-bkg method led to more biases in concentration calculations than the syn-bkg using CLS models. For instance, the zap-bkg underestimated N_2O concentrations by a least 9%, and the syn-bkg improved the quantitative accuracy (Fig. 5 shown in the manuscript). Simply removing the gas absorption feature by the linear function potentially resulted in biases. Thus, applying the PLS to quantify gas concentration from the spectra converted by zap-bkg is unlikely to improve the quantitative accuracy. For simplification, the results of the integrated uses of the zap-bkg and PLS model were not reported. Also, since we were limited to acquire wet CO_2 reference spectra (CO_2/H_2O mixing spectra), the PLS model was not used for CO_2 quantification.

13. General comment: Time series on GHG concentrations at S-OPS including measured ambient air conditions (to have an idea about the variability of wind speed, direction, air temp, etc.) would be helpful.

Response: Information of the environmental variables was updated in supplementary materials (supplementary figure 1) and in figure-7.

14. Fig.7(b) is strange. As stated in the Fig.7(b), bias = FTIR – S-OPS. According to this formula, the bias between 11/6/2014 and 12/6/2014 is negative, since the FTIR concentrations are clearly lower than S-OPS. But in the figure the corresponding bias is positive.

Response: The right Y-axis of bias (%) of figure-7 is reverse, so the biases should be negative. The concentrations of N_2O (ppbv) and CO_2 (ppmv) measured by the S-OPS and OP-FTIR spectra needed to be corrected by the humidity content in the air (dry air correction). The original Figure-7 showed the dry-air corrected concentrations of N_2O and CO_2; however, CO_2 concentrations calculated from OP-FTIR were not corrected by humidity content by accident. The new Figure-7 with the dry-air corrected CO_2 concentrations (FTIR-CO_2) were updated in the manuscript.

Part-II: A list of relevant changes

Summary – Some unclear or ambiguous sentences and paragraphs were rephrased to improve understandings of this paper. The marked-up version of this article was attached (Part-III), and the list of the important changes is as follows:

1. **Article title**: The title was changed to 'Application of Open Path Fourier Transform Infrared Spectroscopy (OP-FTIR) to Measure Greenhouse Gas Concentrations from Agricultural Fields'.

2. **Affiliations**: The 'Department of Earth, Atmospheric and Planetary Sciences, Purdue University, West Lafayette, IN 47907' was added to one of Cliff T. Johnston's affiliations.

3. **Abstract (page 1, line 12)**: Changed the sentence of '… measure concentrations of greenhouse gases (e.g., N_2O and CO_2) emitted from agricultural soils …' to '… measure concentrations of N_2O and CO_2 at a maize cropping system …".

4. **Introduction (Page 2, line 19)**: Briefly introduced the eddy covariance based on suggestions from the Anonymous Referee #3 by adding sentences of 'It is worth mentioning that the eddy covariance flux measurement method, one of the most common micro-meteorological techniques used to investigate gas exchanges in the agroecosystem, is capable of measuring gas fluxes frequently with an increased footprint (Baldocchi, 2003). A large-scale flux measurement (hundred meters to several kilometres) using this method, however, make comparisons among field-scale treatments (1-5 ha) more difficult than chamber methods (Schmid, 1994; Denmead, 2008).'

5. **Materials and experimental methods (Page 5, line 4)**: Rephrased the original sentence to 'Gas samples were drawn through an S-OPS line by a sampling pump in the GSS at approximately 7 $L \cdot min^{-1}$ and collected into a

Teflon® ambient pressure chamber. Then, N_2O and CO_2 analysers drew air samples from the ambient pressure chamber to measure the 'actual' path-averaged concentrations of N_2O and CO_2 along the OP-FTIR path (Heber et al., 2006). The measured N_2O/CO_2 concentrations were used to benchmark concentrations calculated from the OP-FTIR spectrum.'

6. **Materials and experimental methods (Page 5, line 22)**: Rephrased the original paragraph of the 2.3 section of 'Overview of ambient temperature and concentrations of N_2O/CO_2/water vapor'.

7. **Materials and experimental methods (Page 5, line 30)**: Rephrased the original sentence to 'A spectra range of 500.0-4000.0 cm^{-1} and a resolution of 0.5 cm^{-1} were selected for spectra acquisition. Each sampled spectrum was acquired by co-adding 64 single-sided interferograms (IFGs) using the AutoQuant Pro4.0 software package (MIDAC Corporation, Irvine, CA).'

8. **Materials and experimental methods (Page 6, line 32)**: Added the sentence of 'Six points within 2050.0-2500.0 cm^{-1} were selected to fit the curvature of the SB spectrum using a polynomial function to create a syn-bkg SB spectrum (Fig. 3b)' to clarify the process used to generate the 'synthetic' SB background in this study, which is also based on suggestions from the Anonymous Referee #2 and #3.

9. **Results and discussion (Page 8)**: Sections-3.2 (Nitrous oxide (338 ppbv)), the first paragraph in section-3.3 (Carbon dioxide (400 ppmv)), and the first two sentences in section-3.4 (Diurnal N_2O/CO_2 estimations) (page 10, line 27-30) were rephrased to improve sentence fluency and clarify ambiguous concepts. Details were shown in the marked-up manuscript.

10. **Figure-2 (Page 17):** The gray bar shown in Figure 2a was aligned to 338±0.3 ppbv, which was suggested by the Anonymous Referee #3.

11. **Figure-7 (Page 22)**: Two changes shown in Figure 7 were (1) the 30-min averages of air temperature and wind speed measured from 9-19 June 2014 were added in the figure, and (2) the CO_2 concentrations measured from the OP-FTIR spectra were not calibrated by the humidity content in the air (dry air correction) in the original figure-7. The dry-air corrected CO_2 concentrations were updated to the new figure-7. This issue was addressed by C-H Lin on 13 Dec. 2018 on the AMTD forum.

Part-III: A marked-up manuscript version

Application of Open Path Fourier Transform Infrared Spectroscopy (OP-FTIR) to Measure Greenhouse Gas Concentrations from Agricultural Fields~~Soils~~

Cheng-Hsien Lin[1], ~~Cliff T. Johnston[1],~~ Richard H. Grant[1], and Albert J. Heber[2], and Cliff T. Johnston[1,3]

[1]Department of Agronomy, Purdue University, West Lafayette, IN 47907, United States
[2]Department of Agricultural and Biological Engineering, Purdue University, West Lafayette, IN 47907, United States
3Department of Earth, Atmospheric and Planetary Sciences, Purdue University, West Lafayette, IN 47907

Correspondence to: Cheng-Hsien Lin (lin471@purdue.edu)

Abstract. Open-path Fourier transform infrared spectroscopy (OP-FTIR) has often been used to measure hazardous or trace gases from the ~~"~~hot~~"~~ point sources (e.g., volcano, industrial or agricultural facilities) but seldom used~~ to measure greenhouse gases (GHGs) from field-scale sources (e.g., agricultural soils) in the field-scale source areas, such as soil emissions~~. Closed-path mid-IR laser-based N_2O, nondispersive-IR CO_2 analysers, and OP-FTIR were used to measure concentrations of N_2O and CO_2 at a maize cropping system during 9-19 June 2014~~OP-FTIR, the close-path mid-IR laser-based N_2O, and the nondispersive-IR CO_2 analyzers were used to measure the concentrations of greenhouse gases (e.g., N_2O and CO_2) emitted from agricultural soils over a period of 9-19th June in 2014~~. To measure N_2O/CO_2 concentrations accurately, we~~We~~ developed a quantitative method of N_2O/CO_2 analysis that minimized ~~the~~ interferences from diurnal changes of humidity and temperature~~ in order to measure N_2O/CO_2 concentrations accurately~~. Two chemometric multivariate models~~ were developed, a~~: classical least squares (CLS) and~~ a~~ partial least squares (PLS), were developed~~respectively~~. This study evaluated various~~different~~ methods to generate the single beam background spectra, and different spectral regions for determining~~to determine~~ N_2O/CO_2 concentrations from OP-FTIR spectra. A standard extractive method was used to measure the 'actual' path-averaged concentrations along an OP-FTIR optical path in situ, as a benchmark to assess the feasibilities of these quantitative methods. Within ~~the~~ an absolute humidity range of 5,000-20,000 ppmv and the temperature of 10-35 ℃, we found that the CLS model underestimated N_2O concentrations (~~Bias~~ bias = -4.9±3.1 %) calculated from OP-FTIR spectra, and the PLS model improved the accuracy of ~~the~~ calculated N_2O concentrations (~~Bias~~ bias = 1.4±2.3 %). The bias of ~~the~~ calculated CO_2 concentrations was -1.0±2.8 % using the CLS model. These methods suggested that environmental variables potentially lead to biases in N_2O/CO_2 estimations from OP-FTIR spectra and may help OP-FTIR users avoid dependency on extractive methods of calibrations~~the changed ambient factors potentially led to biases in N_2O/CO_2 estimations from OP-FTIR spectra, and may help the OP-FTIR user to escape from the dependency of extractive methods used to calibrate the concentration determined by OP-FTIR~~.

1 Introduction

Agriculture contributes a substantial amount of greenhouse gas (GHG) emissions (e.g. N_2O, CO_2, and CH_4) to the global GHG budget (IPCC, 2007; Cole et al., 1997; Smith et al., 2008). Among these gases, N_2O is mainly emitted from agricultural soils, accounting for 38% of the global anthropogenic non-CO_2 GHG emissions from agricultural activities (US-EPA, 2006; Smith et al., 2007~~; US-EPA, 2006~~). Nitrous oxide~~N_2O~~ is produced from biological reactions that transform available N in soils via microbial nitrification and denitrification (Mosier et al., 2004). Considering~~Taking into account~~ that the global warming potential value of N_2O is 310, it is estimated that overall GHG emission from soils (based on CO_2 equivalents) is approximately 2500 $MtCO_2$-eq yr^{-1}. A significant fraction of soil N_2O emissions results from the use of nitrogen (N) fertilizers in agricultural soils. In addition to contributing to the overall GHG burden of the atmosphere, N_2O emissions also represent a direct loss of ~~the~~ N applied to the field, contributing to the decreased nitrogen use efficiency (NUE) (Eichner, 1990; Ryden and Lund, 1980; Bremner et al., 1981; Omonode et al., 2017). Also, soils play the role of a sink or a source for ~~the~~ atmospheric CO_2 (Paustian et al., 1997; Smith et al., 2008). Changing land use of crop production, especially agricultural-related uses such as tile drained and tilled managements, and agricultural lime application (e,g., $CaCO_3$ and $MgCa(CO_3)_2$) potentially become a large source of CO_2 released to the atmosphere via microbial decomposition of soil organic carbon (Smith, 2004; IPCC, 2007; Cole et al., 1997, West et al., 2005).

The flux chamber~~Chamber~~ measurement~~s have~~ has been the most common method to measure GHG emissions from soils (Denmead, 2008; Rochette and Eriksen-Hamel, 2008). Chamber measurements, however, are subject to significant limitations that lead to uncertainties and biases in ~~the~~ estimated GHG emissions. For instance, because chambers have a small footprint (~0.5 m^2) and generally wide sampling intervals (usually once to twice a week), they are poorly suited for evaluating ~~to study the~~ spatial and temporal variability of GHGs from agricultural soils (Laville et al., 1999; Rowlings et al., 2012; Schelde et al., 2012). Also, ~~the increased~~ wind turbulence is known to substantially induce~~substantially induced~~ more gas transportation from soils to the atmosphere. Chamber methods do not take this~~unlikely consider the~~ wind-induced effect into account, and this likely results~~so likely resulting~~ in underestimations for gas measurements (Denmead and Reicoshky, 2003; Poulsen et al., 2017; Pourbakhtiar et al., 2017). It is worth mentioning that the eddy covariance flux measurement method, one of the most common micro-meteorological techniques used to investigate gas exchanges in the agroecosystem, is capable of measuring gas fluxes frequently with an increased footprint (Baldocchi, 2003). A large-scale flux measurement (hundred meters to several kilometres) using this method, however, make comparisons among field-scale treatments (1-5 ha) more difficult than chamber methods (Schmid, 1994; Denmead, 2008).

Open-path Fourier transform infrared spectroscopy (OP-FTIR) is a non-intrusive sensing approach and capable of detecting multiple components simultaneously, acquiring real-time data at a relatively high temporal resolution (second to minutes), and providing path-averaged gas concentrations (Russwurm and Childers, 1996~~Russwurm et al., 1991~~). OP-FTIR has been

applied to ~~measure~~ measuring atmospheric gases since the 1970s (e.g., hazardous air pollutants, fugitive volatile organic compounds (VOCs), and trace gases) (Herget and Brasher, 1980; Gosz et al., 1988; Russwurm et al., 1991; Bacsik et al., 2006; Briz et al., 2007; Lin et al., 2008). More recently, OP-FTIR has been increasingly applied to measure GHGs or other trace gases in agriculture, mostly in animal facilities (e.g., N_2O, CO_2, CH_4, and NH_3 from the swine or dairy production ~~facility~~) (Childers et al., 2001; Loh et al., 2008; Bjorneberg et al., 2009; Barrancos, 2013; Naylor et al., 2016). Only a few studies, however, implemented OP-FTIR to measure gas emissions from vegetable production fields or fertilized soils (Bai et al., 2014 and 2018; Ni et al., 2015). Integrating OP-FTIR with ~~the~~ micrometeorological techniques (e.g., flux gradient ~~(FG)~~ or backward Lagrangian stochastic dispersion ~~(bLS)~~ methods) can measure gas fluxes from the field-scale source of interest with high temporal and spatial representatives that are less prone to artifacts induced by point-based sampling (Flesch et al., 2004 and 2016; Bai et al., 2014 and 2018; Ni et al., 2015). Moreover, the OP-FTIR combined with a scanning system can potentially be applied to horizontally or vertically survey numerous fields of interest and measure their gas emissions simultaneously (Flesch et al., 2016).

Despite these advantages, OP-FTIR also faces a number of challenges. In order to resolve the spectral features of GHGs, high spectral resolution (< 0.5 cm^{-1}) is required to resolve the rotation-vibrational absorption bands of the GHGs of interest (Griffiths and de Haseth, 2007). Calculating concentrations from FTIR spectra requires both a 'sample' single beam spectrum and a reference/background spectrum that does not contain spectral contributions from GHGs of interest, which is not possible at the field scale (e.g., evacuation of the field); thus, mathematical methods have been developed which strip the spectral bands from a 'sample' single beam spectrum. This challenge requires the use of instrumental- or spectral-processing methods to create a background spectrum, and these methods are subject to biases to determine GHG concentrations (Griffiths and de Haseth, 2007; Russwurm and Childers, 1996). Furthermore, the atmosphere contains the high concentration of water vapour that interferes with the detection and quantification of GHGs of interest (Russwurm and Childers, 1996; Horrocks et al., 2001; Briz et al., 2007; Smith et al., 2011). These challenges of data processes and the interferences from water vapour likely introduce~~d~~ biases and uncertainties in ~~the~~ GHG quantification. Using ~~the~~ error-prone concentration in flux prediction models (micrometeorological techniques) possibly leads to unknown uncertainties in ~~the~~ estimated gas fluxes. Thus, it is essential to develop a comprehensive quantitative method to improve and assure the quality of gas quantification using OP-FTIR.

Testing the feasibility of quantitative methods and qualities (accuracy and precision) of OP-FTIR is challenging because a reliable~~trustable~~ reference is required to validate ~~the~~ FTIR-derived concentrations. One of the most common approaches was to position a gas cell filled with known gas concentrations of interest in the optical path and test their quantitative methods (Russwurm et al., 1991; Horrocks et al., 2001; Smith et al., 2011). This approach, however, somewhat controlled the environment and neglected the effect of ~~the~~ ambient interferences, such as water vapour, on the quality of gas quantification. The alternative approach is to compare the derived concentrations with ambient concentrations. The ambient concentration

of a gas of interest can be determined by averaging the global background concentrations (e.g. N_2O~310 ppbv or CO_2~400 ppmv) or measured from the gas samples that were collected along the OP-FTIR path and ~~analysed~~ analysing their concentrations using laboratory-based~~Lab based~~ gas chromatography (GC) (ASTM, 2013; Childers et al., 1995; Kelliher et al., 2002; Bai et al., 2014). The experimental designs of these assessment approaches, either the point sampled setup or the low sampled frequency or both, became the major problem for cross-validating their OP-FTIR quantitative methods. Since the ambient concentrations likely fluctuate from place to place (e.g., different land uses) and ~~in~~ at different timing (e.g., diurnal or seasonal variation), the spatial and temporal variations of the ambient concentration were potentially misconceived as ~~"~~"bias"~~"~~ in gas quantification. Up to now, only three studies continuously measured ~~the~~ real-time ambient concentration to logically cross-validate ~~their~~ quantitative methods ~~as well as~~and data qualities under ~~the~~ fluctuat~~ed~~ing environmental factors (e.g., the dynamic water vapour), but none of the prior studies actually assessed their methodologies~~assess the methodology~~ for quantifying N_2O concentrations (Briz et al., 2007; Reiche et al., 2014; Frey et al., 2015~~Frey et al., 2015; Reiche et al., 2014~~).

Therefore, the objectives of this study were to 1) develop a long-path gas sampling system that can continuously collect numerous gas samples simultaneously along an ~~optic~~ optical path of OP-FTIR ~~simultaneously~~ and measure ~~the~~ path-averaged concentrations to evaluate ~~the~~ quantitative qualities of N_2O/CO_2 concentrations ~~that were~~ derived from OP-FTIR spectra, and 2) optimize the quantitative method, including post-data processing, analytical window selections, and chemometric multivariate algorithms, ~~(i.e., classical least square and partial least square),~~ that ~~was~~ is less sensitive to ~~the~~ interference of ambient ~~factors (i.e.,~~ humidity and temperature~~,)~~ and capable of determining N_2O and CO_2 concentrations accurately.

2 Materials and experimental methods

2.1 Site description

This study was conducted at the Purdue University Agronomy Center for Research and Extension near West Lafayette, Indiana, the United States (86°56´ W, 40°49´ N, elevation 215 m). The experimental site was located between two fields (~3.5 ~~hectares~~ ha ~~in each~~per field) with a continuous corn system since 2013. Gas measurements began just after the anhydrous ammonia application with total N rate of 220 kg NH_3-N ha^{-1} on 9 June~~ 9th~~ and ended on 19 June~~ 2014~~~~19th~~. The soils were classified as Drummer silty clay loam (fine-silty, mixed, mesic Typic Endoaquoll) with ~~the~~ a bulk density of 1.6 $g \cdot m^{-3}$, organic matter of 3.4 %, soil pH of 6.0, and cation exchange capacity of 23 $cmol_c \cdot kg^{-1}$ (0-20 cm). During 9-19 June~~ 9-19th~~, the cumulative precipitation was 57 mm, and the average soil temperature and moisture from the depth of 0-10 cm were 23±3 °C and 0.32±0.06 $cm^3 \cdot cm^{-3}$~~23(±3) °C and 0.32(±0.06) $cm^3 \cdot cm^{-3}$~~, respectively, which were determined by the on-site weather station.

2.2 Instrumentation setup ~~(Fig.1)~~

The spectrometer was ~~used~~ a ~~MIDAC Corporation~~ monostatic open path FTIR air monitoring system (~~MIDAC~~ Model2501-C, MIDAC Corporation, Irvine, CA). This instrument included the IR source, interferometer, transmitting/receiving telescope, mercury cadmium telluride (MCT) detector and ZnSe optics. A mid-IR beam in the spectrometer passed through the atmosphere along an optical path and returned to the telescope after reflection from a retro-reflector to collect spectra that included ~~the~~ information ~~of~~ about the gas of interest. A cube-corner retroreflector with 26 cubes was mounted on a retractable tripod with 150 m physical path length from the telescope, corresponding to an optical path length of 300 m (Fig. 1).

Ambient concentrations of N_2O and CO_2 were also determined independently to assess the bias and precision. A difference frequency generation (DFG) mid-IR laser-based N_2O/H_2O ~~analyzer~~ analyser (IRIS 4600, Thermo Fisher Scientific Inc., Waltham, MA) and the non-dispersive infrared (NDIR) spectrometer CO_2/H_2O gas ~~analyzer~~ analyser (LI-840, LI-COR Inc., Lincoln, NE) were used to measure N_2O and CO_2 concentrations of the sampled gases from a synthetic open path gas sampling system (S-OPS) (Fig.1). The DFG laser-based N_2O ~~analyzer~~ analyser determined N_2O concentrations in the mid-infrared wavelength with high precision of < 0.15 ppbv (1σ, 3 min~~ute~~ averaging). An NDIR CO_2 ~~analyzer~~ analyser ~~provided~~ exhibited ~~the~~ high accuracy (< 1.5 % of reading) and low noise (< 1.0 ppmv) to determine CO_2 concentrations using a single path, dual~~-~~wavelength, and infrared detections system.

A 50~~-~~m long S-OPS combined with a gas sampling system (GSS) was used to collect gas samples along an optical path of OP-FTIR. An S-OPS consisted of 9.5-mm~~3/8 inch~~ diameter Teflon® tubes and ten inlets fitted with 1.0-µm~~one µm~~ Teflon® filters. The inlet flow rates ~~of each inlet was~~were adjusted by critical orifices ~~in the inlets~~ to 0.70 L·min^{-1} (±10 %). Gas samples were drawn through an S-OPS line by a sampling pump in ~~this~~ the GSS ~~system~~ at approximately 7 L·min^{-1} and collected into a Teflon® ambient pressure chamber. Then, N_2O and CO_2 analys~~z~~ers drew air samples from the ambient pressure chamber to measure the 'actual' path-averaged concentrations of N_2O and CO_2 along the OP-FTIR path (Heber et al., 2006). The measured N_2O/CO_2 concentrations were used to benchmark concentrations calculated from the OP-FTIR spectrum. Temperature, relative humidity, and pressure in the ambient pressure chamber were also recorded every 30 s to monitor the performance of the GSS~~path-integrated air samples from the ambient pressure chamber (Heber et al., 2006), and the "actual" path-averaged concentrations of N_2O and CO_2 along the OP-FTIR path, which was used to benchmark N_2O/CO_2 concentrations calculated from the OP-FTIR spectrum. Temperature, relative humidity, and pressure in the ambient pressure chamber were also recorded every 30 seconds to monitor the functionality of the GSS~~.

Meteorological measurements of air temperature~~,~~ and relative humidity were measured using an HMP45C probe (~~HMP45C,~~ Vaisala Oyj, Helsinki, Finland) at 1.5-m above ground level (a.g.l.).~~, and barometric pressure (278, Setra, Inc., Boxborough,~~

MA) were at 1.5 m height of the mast located next to the S-OPS. The meteorological data were collected by a data logger (Model CR1000, Campbell Scientific, Logan, Utah), and averaged every 10 minutes30 min. Wind speed and direction were acquired from a 3D sonic anemometer (Model 81000, RM Young Inc., Traverse City, MI) mounted at 2.5 m height on the meteorological mast and recorded at 5 min16 Hz intervals. The recorded data were telemetered to the on-site instrumentation trailer.

2.3 Overview of ambient temperature and concentrations of N_2O/CO_2/water vapourGeneral overview of N_2O/CO_2/water vapour concentrations, and air temperature

Figure 2 shows theThe 30-min averaged averages concentrations of ambient N_2O and CO_2 concentrations were determined by measured from the S-OPS, and water vapour content and air temperature were measured at from the meteorological station (Fig.2). during the period of 9-19th June in 2014. During this time intervalthe test, 877 793 valid OP-FTIR spectra were collected with known concentrations of N_2O, CO_2, water vapour, and air temperature were collected. Ninety spectra containing 338±0.3 ppbv N_2O and ninety-three spectra containing 400±3.0 ppmv CO_2 were selected from these valid spectra to calculate concentrations of N_2O and CO_2, respectively, using different quantitative methods.To avoid the non-linear response of absorbance to the wide range of gas concentrations (Lamp et al., 1997), we selected ninety spectra containing 338±0.5 ppbv N_2O and ninety three spectra containing 400±5 ppmv CO_2 which were measured from the S-OPS. These group of spectra with consistent N_2O/CO_2 concentrations but covered by broad ranges of water vapour content and air temperature were used to examine the effect of water vapour and temperature on concentration calculationscovered broad ranges of water vapour content and air temperature. N_2O and CO_2 concentrations were calculated from these selected spectra using different quantitative methods.

2.4 OP-FTIR data acquisition and QA/QC procedure

A spectra range of 500-4000 cm^{-1} and a resolution of 0.5 cm^{-1} were selected for spectra acquisition. Each sampled spectrum was acquired by co-adding 64 single-sided interferograms (IFGs) at a nominal resolution of 0.5 cm^{-1}, which accounted for 32,000 data points were collected with the interval of 0.241 wavenumbers between data points, using the AutoQuant Pro4.0 software package (MIDAC Corporation, Irvine, CA). The IFGs were converted to single beam (SB) spectra using a zero-filling factor of 1, triangular apodization, and Mertz phase correction. A stray light SB spectrum was also acquired by daily pointing the transmitting/receiving telescope away from the retroreflector at the beginning of the experiment every day using the same parameters (Russwurm and Childers, 1996). Each sampled SB spectrum was stray-light corrected by subtracting the stray-light SB spectrum from the sampled SB spectrum before converting to the absorbance spectrum.

The IFGs and corresponding SB spectra were influenced by ambient factors that included wind-derived vibrations, scintillation induced by air mixing, water vapour content, dust accumulation and condensation on the retro-reflector. Criteria of quality assurance were based on the inspection of the IFG and the SB spectrumspectra, followingwhich are followed the

standard guideline in the MIDAC instrumentation manual and the FTIR open-path monitoring guidance documents (Russwurm and Childers, 1996) with the supplement criteria published by Childers et al. (2001b) and Shao et al. (2007) to acquire the high-quality spectra~~um~~. The maximum and minimum of the IFG centerburst ~~of the IFG~~ were controlled between approximately 0.61~~-~~ and 1.14 ~~Volts~~ VDC based on the physical path length of 150~~-~~ m. Any IFG centerburst signals > 2.25 ~~Volts~~ VDC were rejected to avoid a non-linear response of the MCT detector.

2.5 Spectral analyses

2.5.1 An absorbance spectrum converted from a single beam (SB) spectrum

~~In order t~~To calculate a concentration for a given solute, a stray-light corrected SB spectrum is ratioed against an SB background spectrum (GHGs-free) to produce an absorbance spectrum from which the gas concentration is determined using the Beer-Lambert law. As discussed earlier, OP-FTIR measurements do not permit the collection of a background spectrum that is 'free' of GHGs. Two different approaches were used in this study to overcome this constraint. Both methods required a 'normal' SB spectrum corresponding to the path length of interest that was then mathematically manipulated to produce a background spectrum. A representative field SB spectrum and the regions of interest for each ~~of~~ GHG~~s~~ are shown in Figure 3(a). For the "zapped" background method, a background (zap-bkg) was obtained by drawing a straight line between two selected points which removed, or 'zapped,' any spectral contributions below the line using OMINC Macro Basic 8.0 commercial software (Thermo Fisher Scientific, Inc.). This is illustrated for the N_2O region of interest in Figure 3(b), with the two points and the line labelled as 'zapped' background. For the zap-bkg method, ~~we selected~~ one quality SB spectrum was selected ~~every day~~ to create a zap-bkg each day, and all of the sampled SB spectra collected from one day were converted to absorbance spectra using this zap-bkg. Another method, referred to as the 'synthetic' background method, was generated from this same original SB spectrum using IMACC software (Industrial Monitoring and Control Corp., Round Rock, TX~~Texas~~). In this case, numerous points in the 'non-absorbing' region of the SB spectrum were selected as 'base points,' and a high-order fitting function was used to construct a background spectrum. An example in the N_2O region is illustrated in Figure 3(b) and is labeled 'synthetic' background (syn-bkg). Six points within 2050-2500 cm^{-1} were selected to fit the curvature of the SB spectrum using a polynomial function to create a syn-bkg SB spectrum (Fig. 3b). The mathematically manipulated SB spectra were used as background files to convert the sampled SB spectra into absorbance spectra (Fig.3c and 3d). For the syn-bkg method, all data points were stored as one data file, and this file was applied to each sampled SB spectrum to create its syn-bkg. Since the selected points determined the curvature of the syn-bkg SB spectrum, it is critical to choose the data points that do not introduce any distortion (e.g. artificial dips and peaks) into ~~the curvature of~~ the syn-bkg. In general, we avoided selecting data points within the absorption feature of interest (e.g. 2170.0-2224.0 cm^{-1} for N_2O analysis), and ~~an adequate~~the number of data points ~~was~~ used to fit the curvature of the SB spectrum was considered adequate ~~as long as we can~~if it produced a smooth function (Russwurm and Childers, 1996). Adding too many data points

may lead to ~~the~~ artificial distortion in a syn-bkg. Because the syn-bkg is one of the recommended methods ~~used in the~~for spectral analysis (ASTM, 2013), ~~this method~~it was used to assess the feasibility of the zap-bkg method.

2.5.2 Gas quantifications: Multivariate models and spectral window selections

Based on the Beer-Lambert law, we used reference spectra to predict gas concentrations from field absorbance spectra. In this study, we used classical least squares (CLS) and partial least squares (PLS) regressions to calculate N_2O and CO_2 concentrations. The details of these two methods are described as follows:~~.~~

CLS prediction model: Each of the reference spectra used in the CLS model only contained one gas component (e.g. N_2O, CO_2, or water vapour), and these reference spectra were generated from the high-resolution transmission molecular absorption (HITRAN) database (Rothman et al., 2005). The CLS model (AutoQuant Pro4.0) predicted gas concentrations from the field absorbance spectra converted using the zap-bkg method. In addition, CLS spectra were also calculated using the IMACC software to predict gas concentrations from the spectra converted by the syn-bkg method. The non-linear function between the actual and predicted gas concentrations of the reference spectra was selected in the CLS model in both quantitative packages.

PLS prediction model: Each of the reference spectra used in the PLS model consisted of~~had~~ multiple gas components (e.g. an N_2O/H_2O mixing spectrum). Gas samples were delivered to a multi-pass gas cell (White cell) with an optical path length of 33~~.~~ ~~-~~m (Model MARS-8L/40L, Gemini Scientific Instruments, CA). Spectra were collected by a laboratory-based FTIR spectrometer (Nexus 670, Thermo Electron Corporation, Palatine, IL), which ~~including~~ included a globar IR source, a KBr beam splitter, and a mercury cadmium telluride High D* (MCT-High D*) detector. The FTIR spectrometer was purged with dry air (-20 ℃ dew point) produced ~~from~~ by a zero air generator (Model 701H, Teledyne, Thousand Oaks, CA). Certified N_2O was diluted with ultra-pure nitrogen gas using a diluter (Series 4040, Environics Inc, CT), and the water vapour content was controlled by a Nafion tube (Perma Pure, Lakewood, NJ) contained within a sealing container of the saturated water vapour. Temperature and humidity were monitored using a ~~Vaisala model HMT 330~~ humidity and temperature transmitter (Model HMT330, Vaisala Oyj, Helsinki, Finland). The N_2O concentrations were diluted from 30 ppmv to 0.30, 0.40, 0.50, 0.60 and 0.70 ppmv and mixed ~~mixing~~ with water vapour to ~~the~~ relative humidity of 20, 40, 60, and 80 % at 303 K. Spectra were acquired at 0.5 cm^{-1} resolution, averaged from 64 sample scans with triangular apodization. A total of 60 spectra of N_2O/H_2O ~~mixing gases~~mixtures were used to build the PLS model using quantitative spectral processing software~~TQ Analyst software Version 8.0~~ (Thermo Fisher Scientific TQ Analyst Version 8.0~~, Inc.~~). In order to avoid over-fitting the models, the optimum of factors used in PLS models were determined by cross-validation and justified by the prediction residual error sum of squares (PRESS) function. The correlation between the known and the PLS-predicted concentrations was used to quantify N_2O from the field absorbance spectrum converted by syn-bkg within given spectral windows.

Spectral window selections: The window selection (Fig. 4) was critical because of the interferences of water vapour. While a broader window contained more information of the gas of interest and potentially improved the spectral fit between the modeled and sampled spectra and the quantitative accuracy, it also included more features of water vapour and led to biases in gas quantifications. On the other hand, a narrow window can minimize the interfering effect of the uninteresting gases but may reduce the spectral information of the targeted gas which lead to biases in gas calculations (e.g. underestimation ~~for the~~of gas quantification). The window used for N_2O quantifications was ~~from~~ 2130.0 to 2224.0 cm^{-1} that mainly includes the absorbance features of N_2O (P-branch) and water vapour, and other regions (W_N1-4 shown in Fig. 4a)~~we also~~ were also selected ~~different regions~~ for calculating N_2O concentrations. For CO_2, the spectral windows of 2070.0-2085.0 cm^{-1} and 722.0-800.0 cm^{-1} (not shown) contains ~~the~~ features of CO_2 and water vapour (Rothman et al., 2005). Multiple windows (W_C1-3 shown in Fig. 4c) were selected to calculate CO_2 concentrations and assess the effect of water vapour on gas predictions~~We selected the multi-windows to calculate CO_2 concentrations and assessed the effect of water vapour on gas predictions~~.

2.6 The accuracy of the FTIR-calculated concentration and statistical analysis

Bias, the relative error between the S-OPS and OP-FTIR measured N_2O/CO_2, indicated the accuracy of the calculated N_2O and CO_2 concentrations using different spectral analyses (i.e. background types, multivariate models, and spectral windows) and can be calculated following Eq. (1):

$$Bias = \frac{(x_i - x_t)}{x_t} \times 100\% \quad (1)$$

, where x_i is the N_2O or CO_2 concentration calculated from the OP-FTIR spectrum, and x_t is the known N_2O or CO_2 concentration measured ~~from~~ by the S-OPS. The calculated concentrations were statistically analysed by ANOVA procedures and protected least significant difference (LSD) was used for multiple comparisons among population mean biases (α=0.05) (SAS 9.3; SAS Institute Inc., 2012).

3 Results and discussion

3.1 Quantitative methods (SB backgrounds, spectral windows, and multivariate models)

Both SB background methods (zap- and syn-bkg)~~, zap-bkg and syn-bkg, respectively,~~ were used to convert the sampled SB spectra to absorbance spectra for gas quantifications. Different windows (W_N1-4 for N_2O and W_C1-3 for CO_2) were used to calculate N_2O/CO_2 concentrations from absorbance spectra using CLS and PLS models~~Various windows were used to calculate gas concentrations from the field measured OP-FTIR spectrum using CLS and PLS models~~. A series of the OP-FTIR spectra acquired from broad ranges of humility (i.e., 5,000-20,000 ppmv water vapour) and temperature (10-35 ℃) were used to calculate N_2O and CO_2 concentrations. Within these ranges, the mean bias (%) indicated the accuracy of the

calculated N_2O or CO_2 and the standard deviation (SD) referred to the sensitivity of the quantitative method to the changed water vapour and air temperature.

3.2 Nitrous oxide (338 ppbv)

Spectral windows that were less interfered by water vapour absorption features generally improved the accuracy of N_2O quantification~~Generally, the accuracy of the calculated N_2O concentration (mean bias) was improved by narrowing the spectral window because of the lessened water absorption features~~. In the CLS model, N_2O concentrations calculated from the absorbance spectra converted by zap-bkg were underestimated by 10.7±2.3 % using the broadest window (W_N1: 2170.0-2223.7 cm^{-1} shown in Fig. 4a) ~~(Fig. 4) led to an underestimate of 10.7(±2.3) % in N_2O calculations from the absorbance spectra that were converted by zap-bkg.~~. This bias was~~and this bias can be~~ reduced using W_N2 (2188.5-2223.7 cm^{-1}) (i.e. bias = -9.1±2.5 % shown in Fig. 5a~~underestimate~~). Likewise, N_2O concentrations derived from the absorbance spectra converted by syn-bkg were underestimated by 8.2±2.6 % using the W_N1 ~~led to an underestimate of 8.1(±2.6) % in N_2O calculations using syn-bkg.~~. ~~and this~~This bias was reduced using W_N3 (2215.8-2223.7 + 2188.5-2204.1 cm^{-1}) (i.e. bias = -5.6±2.6 % shown in Fig. 5b~~underestimate~~). Although interferences of water vapour can be mitigated by narrowing down ~~the~~ spectral windows ~~mitigated the features as well as interferences of water vapour~~, the narrowest window (W_N4: 2188.5-2204.1 cm^{-1}) used in the CLS model resulted in greater biases than the W_N3 in both zap- and syn-bkg procedures (Fig. 5a and 5b)~~it also lost the information of N_2O and potentially resulted in a great bias to predict N_2O concentrations if the analytical window was over confined~~. The narrowed window also lost N_2O absorption features and presumably increased biases if the analytical window was over confined~~The most confined window (W_N4: 2188.5-2204.1 cm^{-1}) used in the CLS model gave rise to greater biases in both zap- and syn-bkg procedures~~. ~~Beside W_N1 (2170-2223.7 cm^{-1}), the~~The P-branch feature of N_2O extended from 2130.0 to 2223.7 cm^{-1}, and this region was also used to~~we also used this entire region to~~ calculate ~~the~~ N_2O concentration. In CLS model, the window of 2130.0-2223.7 cm^{-1} showed the minimum mean bias of -0.4 % of the calculated N_2O concentrations using syn-bkg (data not shown); however, this window was sensitive to interfering~~a~~ water vapour ~~interference~~ and led to the highest variability in N_2O estimations (i.e., -0.4±5.3 %).

As previously mentioned, it was important~~crucial~~ to generate a reasonable background for the spectral analysis. ~~The N_2O concentration calculated from the absorbance converted by syn-bkg was more accurate than zap-bkg (Fig. 5).~~ In the CLS model, the bias of N_2O quantification~~the calculated N_2O concentration~~ using the syn-bkg was significantly lower than the zap-bkg based on the same spectral window (W_N1-3; ~~P values~~p < 0.05) (Fig. 5a and 5b~~Fig. 5~~). ~~For N_2O quantification, we only used the P-branch of N_2O (2130-2223.7 cm^{-1}) to calculate N_2O concentrations because the R-branch feature of N_2O (2224-2280 m^{-1}) was strongly overlapped by the feature of CO_2 (2224-2450 cm^{-1}) in field spectra. Syn-bkg better simulated the appropriate SB background over P- and R-branches of N_2O than zap-bkg which simply removed the P-branch of N_2O. Thus, syn-bkg can generate the N_2O absorbance (P-branch) without losing N_2O absorbance intensity (Fig. 3d) as well as the accuracy of the calculated N_2O.~~

The syn-bkg method ~~, and~~coupled with the integrated window of 2215.8-2223.7 cm^{-1} and 2188.7-2204.1 cm^{-1} (W_N3) were considered as the optimal combination for N_2O quantifications using ~~the~~ CLS models (i.e., lowest bias = -5.6±2.6 % in CLS~~,~~ shown in Fig.5b). This optimal combination was also used in the PLS model to predict N_2O concentrations. The mean bias of the calculated N_2O was reduced from -5.6 % (CLS model) to -0.3 % (PLS model) (Fig. 5b and 5c). As compared to the CLS model, the PLS model significantly improved the accuracy of N_2O quantification~~the calculated N_2O~~ (~~P~~ p < 0.05) presumably because the PLS algorithm can extract useful latent factors from the N_2O/H_2O mixing spectra (e.g. the contribution of water vapour to N_2O). ~~The PLS model, however, led to higher variability in the calculated N_2O than the CLS model based on the same window (Fig. 5c), indicating that the PLS model was more sensitive to the changed environment than the CLS model.~~

3.3 Carbon dioxide (400 ppmv)

For CO_2 estimations, three spectral windows were used in the 2070.0-2085.0 cm^{-1} range (Fig. 4c). The accuracy of CO_2 quantification~~the calculated CO_2 concentrations~~ was also improved by narrowing the spectral window (Fig. 6). In the CLS model, CO_2 concentrations calculated from the absorbance spectra converted by zap-bkg were underestimated by 6.4±4.1 % using the broadest window (W_C1: 2070-2084 cm^{-1}) ~~led to an underestimate of 6.4(±4.1) % in CO_2 calculations using zap-bkg~~. This bias was reduced by ~~narrowing~~ the narrowed ~~the~~ window ~~to~~ of W_C2 (2075.5-2084.0 cm^{-1}) (i.e. bias = -0.1±4.2 % shown in Fig. 6a ~~underestimate~~). The bias of the calculated CO_2 concentrations~~The calculated bias of CO_2 concentrations~~ was -4.7~~(~~±2.4~~)~~ % using W_C1 ~~and~~ coupled with syn-bkg and reduced to -0.3±2.4 % using W_C2 (Fig. 6b). ~~This bias can be reduced to -0.3(±2.4) % using W_C2.~~ The most confined window (W_C3: 2075.5-2080.5 cm^{-1}) resulted in greater biases than W_C2, and particularly in conjunction with zap-bkg (i.e. bias = 3.2±3.4 % ~~bias~~ shown in Fig. 6a) ~~(Fig. 6)~~. Thus, the range from 2075.5 to 2084.0 cm^{-1} (W_C2) was ~~considered as~~ the optimal window for CO_2 quantification using the CLS model~~estimations~~ (Fig. 4c).

The zap-bkg led to a greater underestimate in N_2O (bias = -10±2.3 % shown in Fig.5a) than CO_2 calculations (bias = -0.1±4.2 % shown in Fig.6a) based on ~~Zap-bkg conjoined with~~ the optimal window (~~i.e.~~ W_N3 or W_C2) used in ~~the~~ CLS models. ~~led to greater underestimates in N_2O than CO_2 calculations (Bias: -10±2.3%, Fig.5a vs. -0.1±4.2%, Fig.6a).~~ Since the absorbance feature~~s~~ of CO_2 at 2076.9 cm^{-1} (the band center) was less complicated than the P-branch of N_2O from 2170.0 to 2224.0 cm^{-1}, the CO_2 absorbance converted by zap-bkg was similar with syn-bkg (Fig. 3c and 3d). Therefore, the calculated bias ~~(Fig. 6)~~ showed that there was no significant difference between zap- and syn-bkg methods for CO_2 concentration calculations using the W_C2 (Fig. 6). ~~Generally speaking, zap-bkg showed a similar trend with syn-bkg by narrowing the spectral window.~~ Zap-bkg, however, led to the higher variability in the calculated CO_2, indicating that simply removing the CO_2 feature by the linear function potentially resulted in biases for CO_2 quantification.

The other potential region for CO_2 quantification was within 722.0-800.0 cm^{-1} (the R-branch of CO_2 ν_2 band~~,~~ shown in Fig. 3a). ~~Various~~ Different windows were examined for calculating~~to calculate~~ CO_2 concentration using the CLS model in this region, and the CO_2 concentrations were underestimated by 40-70 % ~~underestimated~~ no matter which window was used in conjunction with zap-bkg. The ~~minimum calculated~~ mean bias was minimized (bias = -9.0±2.9 %) by using~~-9.0(±2.9) % by incorporating~~ two windows of 723.0-727.7 cm^{-1} and 732.0-738.5 cm^{-1} in conjunction with syn-bkg (data not shown). As compared with the results from the 2070.0-2084.0 cm^{-1} range (Fig. 4c), the 722.0-800.0 cm^{-1} window resulted in a significant underestimation~~s in~~ of CO_2 calculations because 1) more water vapour features interfered with the R-branch of CO_2 features in the 722.0-800.0 cm^{-1} range than CO_2 in the 2070.0-2084.0 cm^{-1} range,~~,~~ and 2) it was difficult to simulate the appropriate background at the low wavenumber region in the SB spectrum.

3.4 Diurnal N_2O/CO_2 estimations

The ~~optimal~~ quantitative approach of leading to the minimum bias in N_2O estimations was to use syn-bkg and W_N3 window in the PLS model (Fig. 5c).~~;~~ For CO_2, only the CLS model was used for calculating concentrations because of missing CO_2/H_2O mixing spectra for PLS models.~~the optimal approach for~~ The approach leading to the minimum bias in CO_2 estimations in this study~~ CO_2 estimations~~ was to use ~~the~~ syn-bkg ~~procedure and~~with the W_C2 window in the CLS model (Fig. 6b). These procedures~~These optimized methods~~ were used to estimate ~~the~~ N_2O and CO_2 concentrations from the OP-FTIR spectra collected from 9~~th~~ to 19~~th~~ ~~in~~ June 2014 (Fig. 7). The diurnal fluctuation in N_2O/~~ and~~ CO_2 concentrations ~~were corresponding~~corresponded to~~ the~~ diurnal changes of ~~the~~ wind speed and air temperature. The higher N_2O/CO_2 concentrations were usually measured during the night because of N_2O and CO_2 accumulations. The accumulation of N_2O/CO_2 occurred near the ground when turbulent mixing was low, resulting from ~~the~~ decreasing buoyancy from the ground surface (i.e. a stable atmosphere). The greater density of air parcels due to ~~the~~ decreasing temperature also led to the gas accumulation. The diurnal variation in CO_2 was greater than N_2O (Fig. 7b), and we hypothesized ~~because of the~~it was due to multiple sources of CO_2. While N_2O was mostly produced from soils via microbial nitrification and denitrification, ~~but~~ CO_2 was emitted via soil respiration (including microbes and corn root) as well as ~~the~~ respiration from grass and corn leaves.

Mixing of the surface layer of~~ the~~ air tended to result in greater homogeneity along the optical path. Under low wind speed, the presumably poorly-mixed air increased the variability of the path-averaged N_2O/CO_2 concentrations along the optical path, resulting in the difference between the 50~~-~~-m S-OPS and the 150~~-~~-m OP-FTIR. The calculated biases of N_2O and CO_2 were 1.3~~(~~±2.6~~)~~ % (n=363) and -0.7~~(~~±5~~6~~.8~~0~~)~~ % (n=327), respectively, while the mean wind velocity ranged from 0.1 to 8.4 $m \cdot s^{-1}$ (Fig. 7). The variability of the calculated biases of N_2O and CO_2 were reduced when the data that were collected in~~under~~ the low wind speeds (<1.7 $m \cdot s^{-1}$) were excluded, i.e. $bias_{N_2O}$ =1.4±2.3 % (n=29~~8~~5) and $bias_{CO_2}$ =-1.0±2.8 % (n=272~~69~~).

4 Conclusion

We have developed and evaluated different~~various~~ methods for quantifying~~to quantify~~ concentrations of nitrous oxide and carbon dioxide using open-path FTIR based on combinations of single beam backgrounds (~~i.e.~~ zap-bkg and syn-bkg), analytical windows (W_N1-4 and W_C1-3), and chemometric multivariate calibration models (~~i.e.~~ CLS and PLS). It is challenging to generate the P-branch N_2O absorbance within 2170.0-2223.7 cm^{-1} to predict N_2O accurately but feasible to generate ~~CO_2~~ absorbance ~~in~~ within 2075.5-2084 cm^{-1} for CO_2 prediction using the zap-bkg method. The principle for selecting spectral windows is ~~to~~ that ~~use~~ using the region with less water vapour features, ~~yet~~ while over confining the analytical region may lead to biases in gas predictions. The CLS model, the most common approach used for gas retrievals in OP-FTIR commercial packages, underestimates N_2O concentrations but ~~can~~ predicts CO_2 accurately within ~~the~~ an absolute humidity range of 5,000-20,000 ppmv and ~~the~~ a temperature range of 10-35 ℃. In this study, the method resulting in the minimum bias~~the optimal method~~ for N_2O quantification is to use the combination of syn-bkg, a two bands window (2188.7-2204.1 + 2215.8-2223.7 cm^{-1}), and the PLS model (N_2O bias = 1.4±2.3 %). The method leading to the minimum bias in~~The optimal method for~~ CO_2 quantification is to use the combination of syn-bkg, 2075.5-2084.0 cm^{-1} window, and the CLS model (CO_2 bias = -1.0±2.8 %). We ~~provide~~ describe comprehensive methods of N_2O/CO_2 analyses for the increasing number of OP-FTIR users who are interested in greenhouse gas emissions from agricultural fields.

Acknowledgments. This study was supported by the United States Department of Agriculture National Institute for Food and Agriculture Grant No. 13-68002-20421, Indiana Corn Marketing Council Grant No. 12076053, Purdue University Climate Change Research Center. We would like to thank Dr. Tony Vyn and Terry West for the crop and field management, and Austin Pearson for data collection and analyses.

References

ASTM International.: ASTM E1865-97(2013) Standard Guide for Open-Path Fourier Transform Infrared (OP/FT-IR) Monitoring of Gases and Vapors in Air, West Conshohocken, PA, doi:10.1520/E1865-97R13, 2013.

ASTM International.: ASTM E1982-98(2013) Standard Practice for Open-Path Fourier Transform Infrared (OP/FT-IR) Monitoring of Gases and Vapors in Air, West Conshohocken, PA, doi:10.1520/E1982-98R13, 2013.

Bacsik, Z., Komlosi, V., Ollar, T., and Mink, J.: Comparison of open path and extractive long-path FTIR techniques in detection of air pollutants, Appl. Spectrosc. Rev., 41, 77-97, doi:10.1080/05704920500385494, 2006.

Bai, M., Suter, H., Lam, S. K., Sun, J. L., and Chen, D. L.: Use of open-path FTIR and inverse dispersion technique to quantify gaseous nitrogen loss from an intensive vegetable production site, Atmos. Environ., 94, 687-691, doi:10.1016/j.atmosenv.2014.06.013, 2014.

Bai, M., Suter, H., Lam, S. K., Davies, R., Flesch, T. K., and Chen, D. L.: Gaseous emissions from an intensive vegetable farm measured with slant-path FTIR technique, Agric. For. Meteorol., 258, 50-55, doi:10.1016/j.agrformet.2018.03.001, 2018.

Baldocchi, D. D.: Assessing the eddy covariance technique for evaluating carbon dioxide exchange rates of ecosystems: past, present and future, Global Change Biology, 9, 479-492, 10.1046/j.1365-2486.2003.00629.x, 2003.

Barrancos, J., Briz, S., Nolasco, D., Melian, G., Padilla, G., Padron, E., Fernandez, I., Perez, N., and Hernandez, P. A.: A new method for estimating greenhouse gases and ammonia emissions from livestock buildings, Atmos. Environ., 74, 10-17, doi:10.1016/j.atmosenv.2013.03.021, 2013.

Bjorneberg, D. L., Leytem, A. B., Westermann, D. T., Griffiths, P. R., Shao, L., and Pollard, M. J.: Measurement of atmospheric ammonia, methane, and nitrous oxide at a concentrated dairy production facility in southern Idaho using open-path FTIR spectrometry, Trans. ASABE, 52, 1749-1756, 2009.

Bremner, J. M., Breitenbeck, G. A., and Blackmer, A. M.: Effect of nitrapyrin on emission of nitrous oxide from soil fertilized with anhydrous ammonia, Geophys. Res. Lett., 8, 353-356, doi:10.1029/GL008i004p00353, 1981.

Briz, S., de Castro, A. J., Díez, S., López, F., and Schäfer, K.: Remote sensing by open-path FTIR spectroscopy. Comparison of different analysis techniques applied to ozone and carbon monoxide detection, J. Quant. Spectrosc. Radiat. Transf., 103, 314-330, doi:10.1016/j.jqsrt.2006.02.058, 2007.

Childers, J. W., Russwurm, G. M., and Thompson, E. L.: Quality assurance considerations in a long-term FTIR monitoring program, Proc. SPIE 2365, Optical Sensing for Environmental and Process Monitoring, doi: 10.1117/12.210812, 1995.

Childers, J. W., Thompson, E. L., Harris, D. B., Kirchgessner, D. A., Clayton, M., Natschke, D. F., and Phillips, W. J.: Multi-pollutant concentration measurements around a concentrated swine production facility using open-path FTIR spectrometry, Atmos. Environ., 35, 1923-1936, doi:10.1016/s1352-2310(00)00545-8, 2001a

Childers, J. W., Thompson, E. L., Harris, D. B., Kirchgessner, D. A., Clayton, M., Natschke, D. F., and Phillips, W. J.: Application of standardized quality control procedures to open-path Fourier transform infrared data collected at a concentrated swine production facility, Environ. Sci. Technol., 35, 1859-1866, doi:10.1021/es001744f, 2001b.

Cole, C. V., Duxbury, J., Freney, J., Heinemeyer, O., Minami, K., Mosier, A., Paustian, K., Rosenberg, N., Sampson, N., Sauerbeck, D., and Zhao, Q.: Global estimates of potential mitigation of greenhouse gas emissions by agriculture, Nutr. Cycl. Agroecosyst., 49, 221-228, doi:10.1023/a:1009731711346, 1997.

Denmead, O., and Reicosky, D.: Tillage-induced gas fluxes: comparison of meteorological and large chamber techniques, Proc. ISTRO, 16, 357-363, 2003.

Denmead, O. T.: Approaches to measuring fluxes of methane and nitrous oxide between landscapes and the atmosphere, Plant Soil, 309, 5-24, doi:10.1007/s11104-008-9599-z, 2008.

Eichner, M. J.: Nitrous Oxide Emissions from Fertilized Soils: Summary of Available Data, J. Environ. Qual., 19, doi:10.2134/jeq1990.00472425001900020013x, 1990.

Flesch, T. K., Wilson, J. D., Harper, L. A., Crenna, B. P., and Sharpe, R. R.: Deducing ground-to-air emissions from observed trace gas concentrations: A field trial, J. Appl. Meteorol., 43, 487-502, doi:10.1175/1520-0450(2004)043<0487:dgefot>2.0.co;2, 2004.

Flesch, T. K., Baron, V. S., Wilson, J. D., Griffith, D. W. T., Basarab, J. A., and Carlson, P. J.: Agricultural gas emissions during the spring thaw: Applying a new measurement technique, Agric. For. Meteorol., 221, 111-121, doi:10.1016/j.agrformet.2016.02.010, 2016.

Frey, M., Hase, F., Blumenstock, T., Gross, J., Kiel, M., Tsidu, G. M., Schafer, K., Sha, M. K., and Orphal, J.: Calibration and instrumental line shape characterization of a set of portable FTIR spectrometers for detecting greenhouse gas emissions, Atmos. Meas. Tech., 8, 3047-3057, doi: 10.5194/amt-8-3047-2015, 2015.

Gosz, J. R., Dahm, C. N., and Risser, P. G.: Long-Path FTIR Measurement of Atmospheric Trace Gas Concentrations, Ecology, 69, 1326-1330, doi:10.2307/1941630, 1988.

Griffiths, P. R., and de Haseth, J. A.: Fourier transform infrared spectrometry, John Wiley & Sons, 2007.

Heber, A. J., Ni, J. Q., Lim, T. T., Tao, P. C., Schmidt, A. M., Koziel, J. A., Beasley, D. B., Hoff, S. J., Nicolai, R. E., Jacobson, L. D., and Zhang, Y. H.: Quality assured measurements of animal building emissions: Gas concentrations, J. Air Waste Manage. Assoc., 56, 1472-1483, doi:10.1080/10473289.2006.10465680, 2006.

Herget, W. F., and Brasher, J. D.: Remote Fourier transform infrared air pollution studies, Opt. Eng., 19, 194508-194508-, doi:10.1117/12.7972551, 1980.

Horrocks, L. A., Oppenheimer, C., Burton, M. R., Duffell, H. J., Davies, N. M., Martin, N. A., and Bell, W.: Open-path Fourier transform infrared spectroscopy of SO_2: An empirical error budget analysis, with implications for volcano monitoring, J. Geophys. Res.-Atmos., 106, 27647-27659, doi:10.1029/2001jd000343, 2001.

Kelliher, F. M., Reisinger, A. R., Martin, R. J., Harvey, M. J., Price, S. J., and Sherlock, R. R.: Measuring nitrous oxide emission rate from grazed pasture using Fourier-transform infrared spectroscopy in the nocturnal boundary layer, Agric. For. Meteorol., 111, 29-38, doi:10.1016/s0168-1923(02)00007-2, 2002.

~~Lamp, T., Radmacher, M., Weber, K., Gartner, A., Nitz, R., and Broker, G.: Calibration of an open-path FTIR spectrometer for methane, ethylene and carbon monoxide using a fixed 20m multipass cell, Remote Sensing of Vegetation and Water, and Standardization of Remote Sensing Methods, edited by: Cecchi, G., Lamp, T., Reuter, R., and Weber, K., Spie - Int Soc Optical Engineering, Bellingham, 126-136 pp., doi:10.1117/12.274748, 1997.~~

Laville, P., Jambert, C., Cellier, P., and Delmas, R.: Nitrous oxide fluxes from a fertilised maize crop using micrometeorological and chamber methods, Agric. For. Meteorol., 96, 19-38, doi:10.1016/s0168-1923(99)00054-4, 1999.

Lin, C., Liou, N., and Sun, E.: Applications of Open-Path Fourier Transform Infrared for Identification of Volatile Organic Compound Pollution Sources and Characterization of Source Emission Behaviors, J. Air Waste Manage. Assoc., 58, 821-828, doi:10.3155/1047-3289.58.6.821, 2008.

Loh, Z., Chen, D., Bai, M., Naylor, T., Griffith, D., Hill, J., Denmead, T., McGinn, S., and Edis, R.: Measurement of greenhouse gas emissions from Australian feedlot beef production using open-path spectroscopy and atmospheric dispersion modelling, Aust. J. Exp. Agric., 48, 244-247, doi:10.1071/ea07244, 2008.

Mosier, A., Wassmann, R., Verchot, L., King, J., and Palm, C.: Methane and Nitrogen Oxide Fluxes in Tropical Agricultural Soils: Sources, Sinks and Mechanisms, Environ. Dev. Sustain., 6, 11-49, doi:10.1023/B:ENVI.0000003627.43162.ae, 2004.

Naylor, T. A., Wiedemann, S. G., Phillips, F. A., Warren, B., McGahan, E. J., and Murphy, C. M.: Emissions of nitrous oxide, ammonia and methane from Australian layer-hen manure storage with a mitigation strategy applied, Anim. Prod. Sci., 56, 1367-1375, 10.1071/an15584, 2016.

Ni, K., Koster, J. R., Seidel, A., and Pacholski, A.: Field measurement of ammonia emissions after nitrogen fertilization-A comparison between micrometeorological and chamber methods, Eur. J. Agron., 71, 115-122, doi:10.1016/j.eja.2015.09.004, 2015.

IPCC. Intergovernmental Panel on Climate Change, Fourth Assessment Report-Working I Report: The physical science basis, Cambridge Univ. Press, Cambridge, 2007.

Omonode, R. A., Halvorson, A. D., Gagnon, B., and Vyn, T. J.: Achieving lower nitrogen balance and higher nitrogen recovery efficiency reduces nitrous oxide emissions in North America's maize cropping systems, Frontiers in plant science, 8, 1080-1080, doi:10.3389/fpls.2017.01080, 2017.

Paustian, K., Andren, O., Janzen, H. H., Lal, R., Smith, P., Tian, G., Tiessen, H., Van Noordwijk, M., and Woomer, P. L.: Agricultural soils as a sink to mitigate CO_2 emissions, Soil Use Manage., 13, 230-244, 10.1111/j.1475-2743.1997.tb00594.x, 1997.

Poulsen, T. G., Furman, A., and Liberzon, D.: Effects of Wind Speed and Wind Gustiness on Subsurface Gas Transport, Vadose Zone J., 16, doi:10.2136/vzj2017.04.0079, 2017.

Pourbakhtiar, A., Poulsen, T. G., Wilkinson, S., and Bridge, J. W.: Effect of wind turbulence on gas transport in porous media: experimental method and preliminary results, Eur. J. Soil Sci., 68, 48-56, doi:10.1111/ejss.12403, 2017.

Reiche, N., Westerkamp, T., Lau, S., Borsdorf, H., Dietrich, P., and Schütze, C.: Comparative study to evaluate three ground-based optical remote sensing techniques under field conditions by a gas tracer experiment, Environ. Earth Sci., 72, 1435-1441, doi:10.1007/s12665-014-3312-8, 2014.

Rothman, L. S., Jacquemart, D., Barbe, A., Benner, D. C., Birk, M., Brown, L. R., Carleer, M. R., Chackerian, C., Chance, K., Coudert, L. H., Dana, V., Devi, V. M., Flaud, J. M., Gamache, R. R., Goldman, A., Hartmann, J. M., Jucks, K. W., Maki, A. G., Mandin, J. Y., Massie, S. T., Orphal, J., Perrin, A., Rinsland, C. P., Smith, M. A. H., Tennyson, J., Tolchenov, R. N., Toth, R. A., Vander Auwera, J., Varanasi, P., and Wagner, G.: The HITRAN 2004 molecular spectroscopic database, J. Quant. Spectrosc. Radiat. Transf., 96, 139-204, doi:10.1016/j.jqsrt.2004.10.008, 2005.

Rochette, P., and Eriksen-Hamel, N. S.: Chamber measurements of soil nitrous oxide flux: are absolute values reliable?, Soil Sci. Soc. Am. J., 72, 331-342, doi: 10.2136/sssaj2007.0215, 2008.

Rowlings, D. W., Grace, P. R., Kiese, R., and Weier, K. L.: Environmental factors controlling temporal and spatial variability in the soil-atmosphere exchange of CO_2, CH_4 and N_2O from an Australian subtropical rainforest, Glob. Change Biol., 18, 726-738, doi:10.1111/j.1365-2486.2011.02563.x, 2012.

Russwurm, G. M., Kagann, R. H., Simpson, O. A., and McClenny, W. A.: Use of a fourier-transform spectrometer as a remote sensor at superfund sites, Proc. SPIE 1433, Measurement of Atmospheric Gases, 302-314, doi: 10.1117/12.46177, 1991.

Russwurm, G. M., Kagann, R. H., Simpson, O. A., McClenny, W. A., and Herget, W. F.: Long-path FTIR measurements of volatile organic-compounds in an industrial-setting, J. Air Waste Manage. Assoc., 41, 1062-1066, doi:10.1080/10473289.1991.10466900, 1991.

Russwurm, G. M., and Childers, J. W.: FT-IR open-path monitoring guidance document, ManTech Environmental Technology, Inc., Research Triangle Park, NC (United States), 1996.

Ryden, J. C., and Lund, L. J.: Nitrous Oxide Evolution from Irrigated Land[1], J. Environ. Qual., 9, doi:10.2134/jeq1980.00472425000900030012x, 1980.

Schelde, K., Cellier, P., Bertolini, T., Dalgaard, T., Weidinger, T., Theobald, M. R., and Olesen, J. E.: Spatial and temporal variability of nitrous oxide emissions in a mixed farming landscape of Denmark, Biogeosciences, 9, 2989-3002, doi:10.5194/bg-9-2989-2012, 2012.

Schmid, H. P.: Source areas for scalars and scalar fluxes, Boundary-Layer Meteorology, 67, 293-318, doi:10.1007/bf00713146, 1994.

Shao, L., Pollard, M. J., Griffiths, P. R., Westermann, D. T., and Bjorneberg, D. L.: Rejection criteria for open-path Fourier transform infrared spectrometry during continuous atmospheric monitoring, Vib. Spectrosc., 43, 78-85, doi:10.1016/j.vibspec.2006.06.016, 2007.

Smith, P.: Carbon sequestration in croplands: the potential in Europe and the global context, Eur. J. Agron., 20, 229-236, doi:10.1016/j.eja.2003.08.002, 2004.

Smith, P., Martino D., Cai Z., Gwary D., Janzen H., Kumar P., McCarl B., Ogle S., O'Mara F., Rice C., Scholes B., and Sirotenko O.: Agriculture. In B. Metz et al. (ed.) Mitigation. Contribution of Working Group III to the fourth assessment report of the Intergovernmental Panel on Climate Change. Cambridge Univ. Press, Cambridge, UK, 2007.

Smith, P., Martino, D., Cai, Z., Gwary, D., Janzen, H., Kumar, P., McCarl, B., Ogle, S., O'Mara, F., Rice, C., Scholes, B., Sirotenko, O., Howden, M., McAllister, T., Pan, G., Romanenkov, V., Schneider, U., Towprayoon, S., Wattenbach, M., and Smith, J.: Greenhouse gas mitigation in agriculture, Philos. Trans. R. Soc. B-Biol. Sci., 363, 789-813, doi:10.1098/rstb.2007.2184, 2008.

Smith, T. E. L., Wooster, M. J., Tattaris, M., and Griffith, D. W. T.: Absolute accuracy and sensitivity analysis of OP-FTIR retrievals of CO_2, CH_4 and CO over concentrations representative of "clean air" and "polluted plumes", Atmos. Meas. Tech., 4, 97-116, doi:10.5194/amt-4-97-2011, 2011.

US-EPA: Global Anthropogenic Emissions of Non-CO_2 Greenhouse Gases: 1990-2020, United States Environmental Protection Agency, EPA 430-R-06-003, Washington, D.C., <https://www.epa.gov/sites/production/files/2016-05/documents/globalanthroemissionsreport.pdf>, 2006.

West, T. O., and McBride, A. C.: The contribution of agricultural lime to carbon dioxide emissions in the United States: dissolution, transport, and net emissions, Agric. Ecosyst. Environ., 108, 145-154, doi:10.1016/j.agee.2005.01.002, 2005.

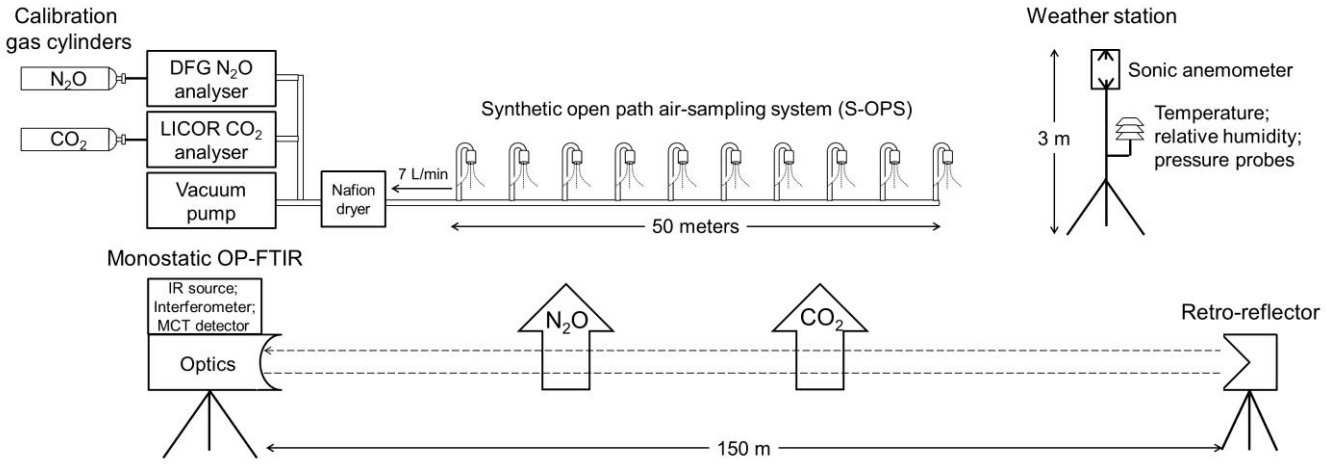

Figure 1. Schematic of the instrumentation used to assess the accuracy of N_2O and CO_2 concentration determined by OP-FTIR in this study. DFG N_2O and LI-840 CO_2 analysers~~analyzers~~ combined with the synthetic open path air-sampling system (S-OPS) were used to measure the 'actual' path-averaged N_2O/CO_2 concentrations and benchmark the N_2O and CO_2 concentrations calculated from OP-FTIR spectral analyses. The humidity, air temperature, and wind information were measured from the weather station.

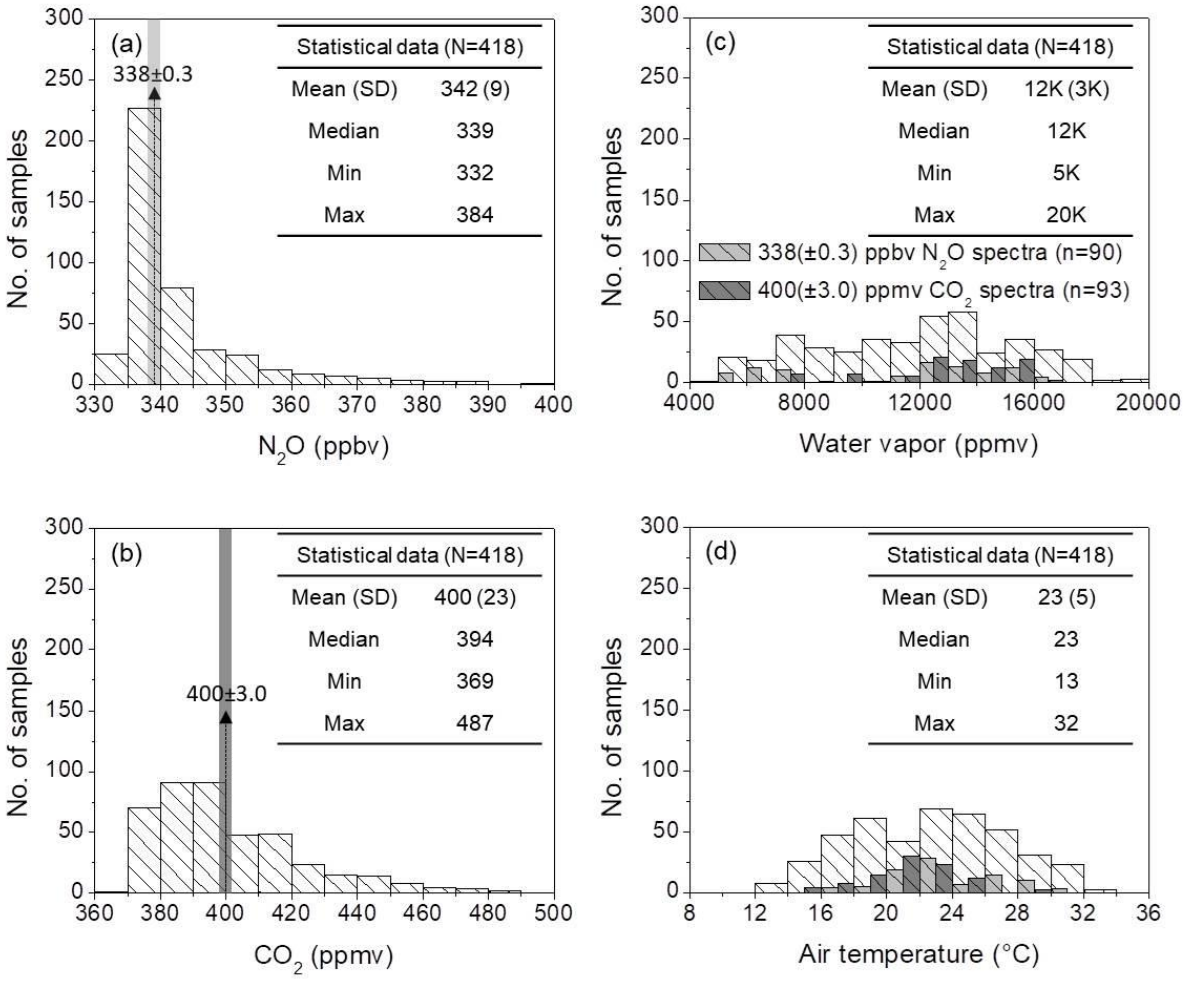

Figure 2. The 30-min averaged concentrations of (a) N_2O and (b) CO_2 were measured using N_2O and CO_2 analysersanalyzers by sampling the air from S-OPS, and the 30-min averages of (c) water vapour content and (d) air temperature were also measured from the on-site weather station during 9th-19th in June, 2014. The concentrations of N_2O, CO_2, and water vapour showed shown in these figures were measured while the air was well-mixing (U > 1.51.7 m·s^{-1}). The light gray bars mean the OP-FTIR spectra containing contained 338(±0.35) ppbv N_2O and the dark gray barks mean the OP-FTIR spectra containing contained 400(±3.05) ppmv CO_2. Both the selected spectra (N_2O 338 ppbv, n=90; CO_2 400 ppmv, n=93) covered the broad ranges of water vapour and air temperature and were used to assess the sensitivity of the OP-FTIR quantitative methods to the dynamic ambient factorsvariables.

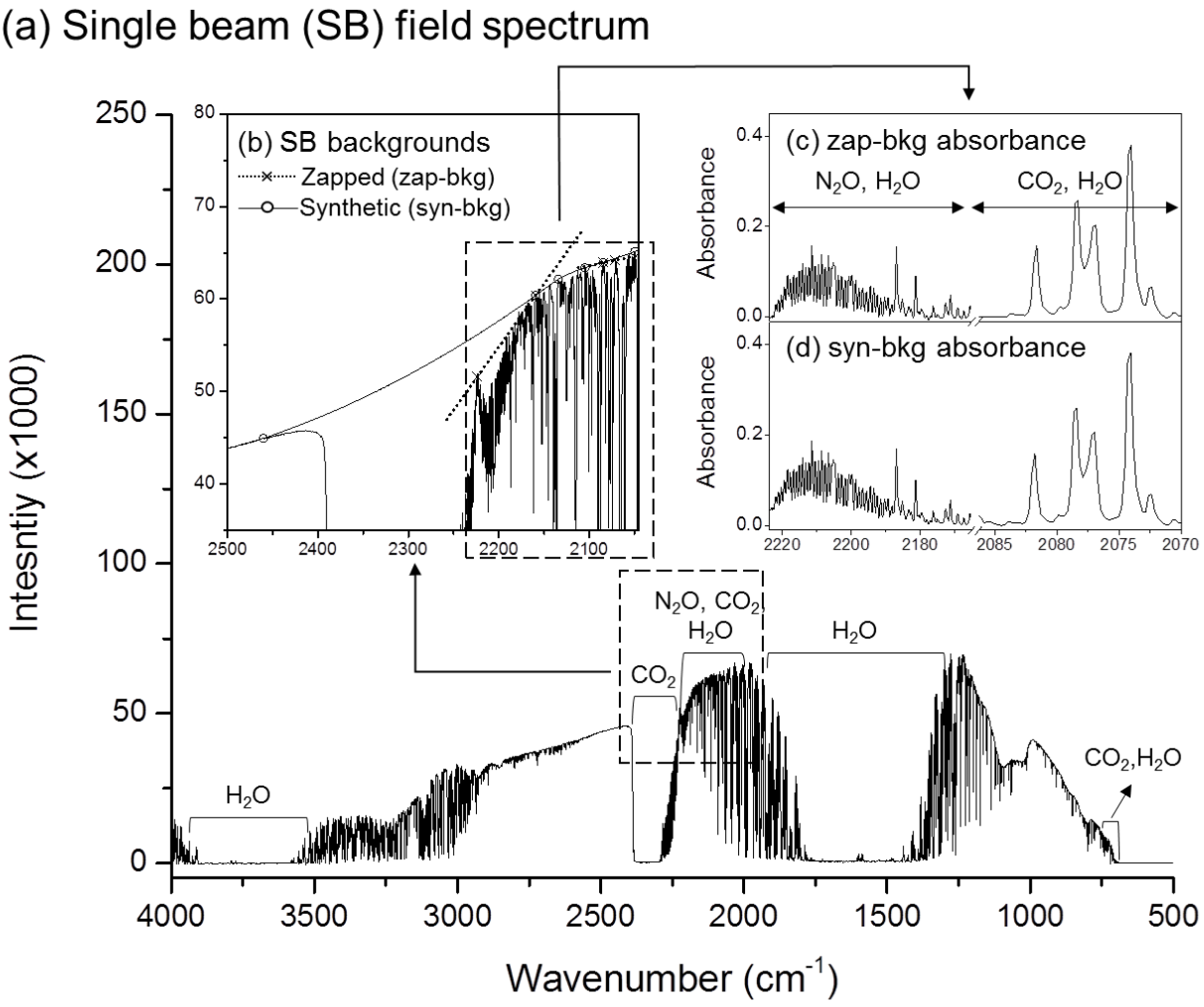

Figure 3. The illustrations of (a) a field single beam (SB) OP-FTIR spectrum containing the regions of N_2O, CO_2, and water vapour was collected through an optical path length of 300 m; (b) ~~a~~ zapped and ~~a~~ synthetic SB backgrounds (zap-bkg and syn-bkg) ~~were~~ generated from this field SB spectrum and used to convert the sampled SB spectrum to (c) the absorbance spectra that allow us to calculate N_2O/CO_2 concentrations using the Beer-Lambert law.

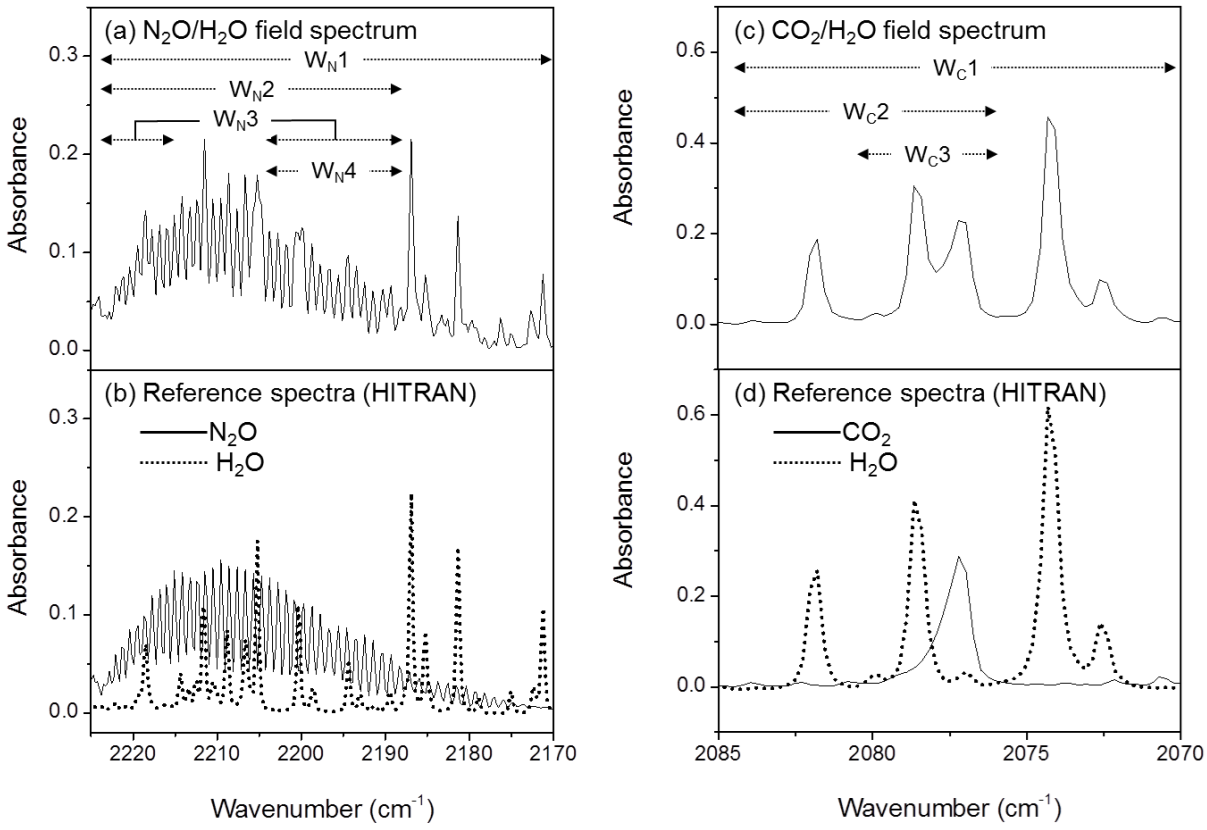

Figure 4. Field and HITRAN reference absorbance spectra: (a) Field spectrum containing the features of N_2O and water vapour, (b) reference spectra of N_2O and water vapour at 2170.0 – ~~2225~~ 2224.0 cm^{-1}, (c) field spectrum containing the features of CO_2 and water vapour, and (d) reference spectra of CO_2 and water vapour at 2070.0 – ~~2085~~ 2084.0 cm^{-1}. W_N(1-4) and W_C(1-3) denote the spectral windows used to calculate N_2O and CO_2 concentrations from field spectra.

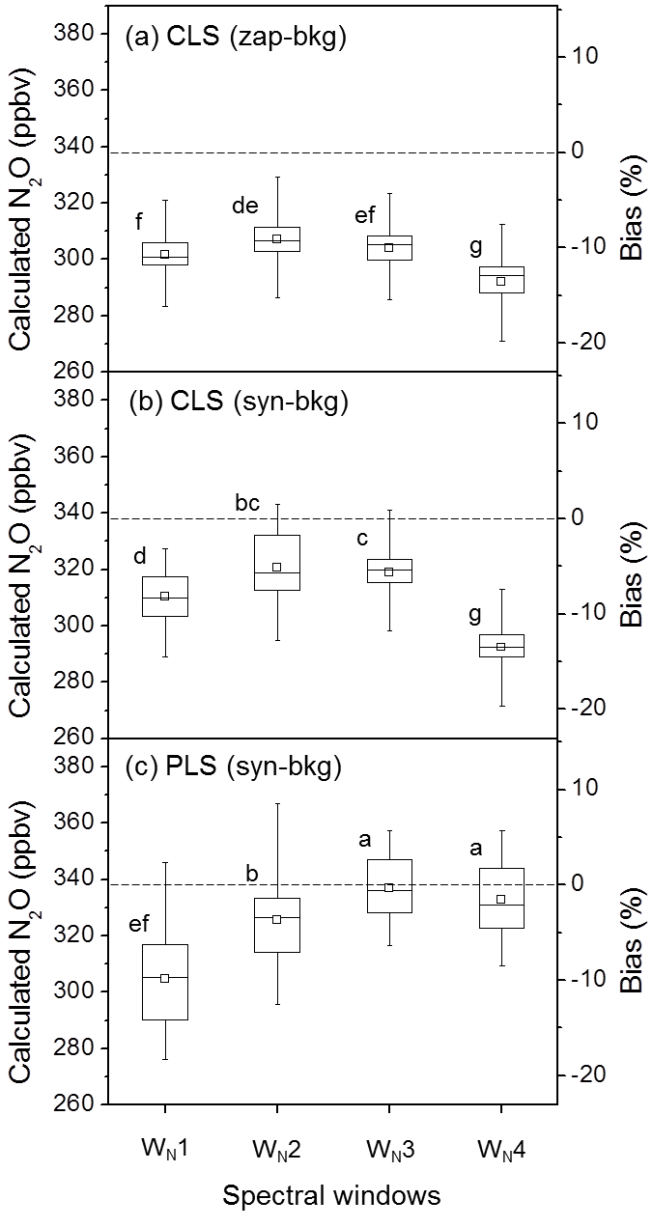

Figure 5. The box plots of the calculated N_2O concentrations and the corresponding biases from a series of OP-FTIR spectra (n=90) that contain 338±0.3 ppbv N_2O with ~~the changed~~varying humidity and air temperature using different SB background-processing methods (~~i.e.~~ zap-bkg and syn-bkg), and four spectral windows (W_N1-4) in the CLS and PLS models: (a) zap-bkg + CLS model, (b) syn-bkg + CLS model, and (c) syn-bkg + PLS model. The plot displays the mean (□), median (—), interquartile ranges (box), and extreme values (whiskers). Different letters indicate ~~the~~ significant differences ($P < 0.05$) among the means calculated by different quantitative methods by the least significant difference (LSD).

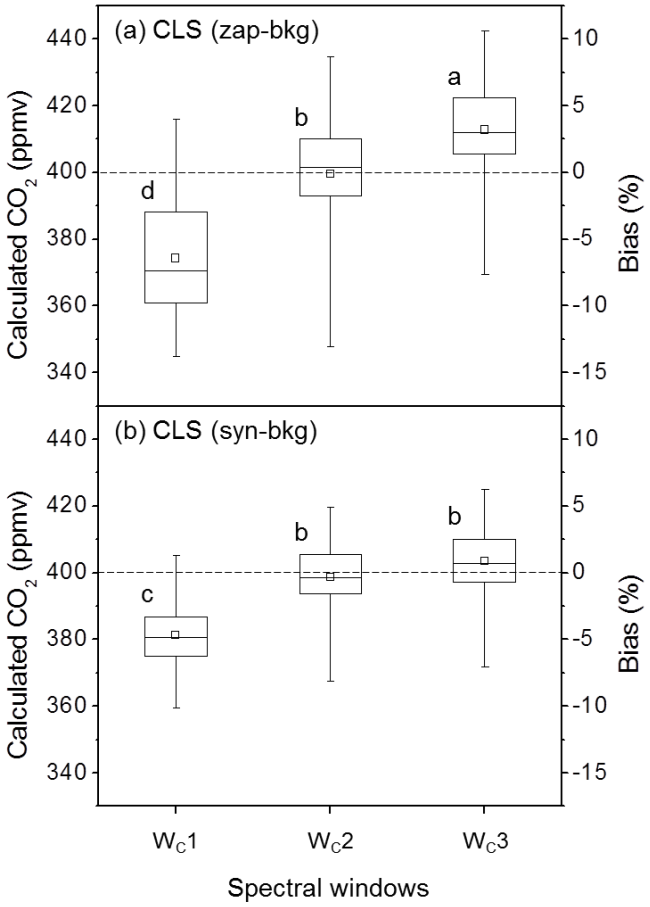

Figure 6. The box plots of the calculated CO_2 concentrations and the corresponding biases from a series of OP-FTIR spectra (n=93) that contain 400±3.0 ppmv CO_2 with ~~the changed~~varying humidity and air temperature using different SB background-processing methods (~~i.e.~~ zap-bkg and syn-bkg), and three spectral windows (W_C1-3) in the CLS model: (a) zap-bkg, and (b) syn-bkg. The plot displays the mean (□), median (—), interquartile ranges (box), and extreme values (whiskers). Different letters indicate ~~the~~ significant differences ($P < 0.05$) among the means calculated by different quantitative methods by the least significant difference (LSD).

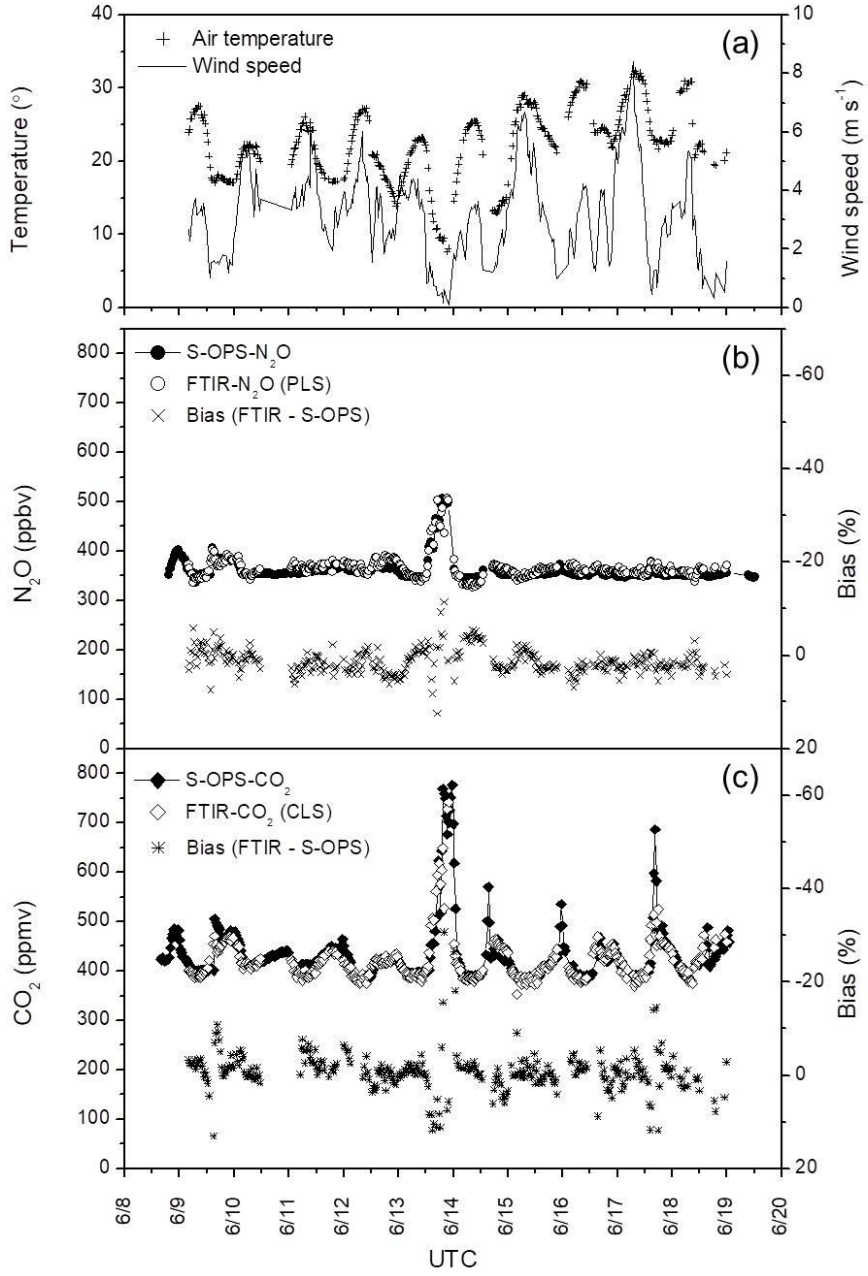

Figure 7. Measurements of air temperature, wind speed, N_2O and CO_2 concentrations from 9-19 June 2014. The 30-min averages of (a) air temperature and wind speed, (b) N_2O concentrations measured from S-OPS using the DFG N_2O analyser and calculated from OP-FTIR using the method of (syn-bkg + W_N3 + PLS), and the corresponding biases, and (c) CO_2 concentrations measured from S-OPS using LI-840 CO_2 analyser and calculated from OP-FTIR using the method of (syn-bkg + W_C2 + CLS), and the corresponding biases~~N_2O and CO_2 concentrations from 9th to 19th in June 2014: (a) N_2O concentrations measured from S-OPS using the DFG N_2O analyzer and calculated~~

~~from OP-FTIR using the optimal methods (syn-bkg + W_N3 + the PLS model), and the corresponding biases, and (b) CO_2 concentrations measured from S-OPS using LI-840 CO_2 analyzer and calculated from OP-FTIR using the optimal method (syn-bkg + W_C2 + the CLS model), and the corresponding bias~~.